GEOPHYSICAL RESEARCH LETTERS, VOL. 20, NO. 19, PAGES 2035-2038, OCTOBER 8, 1993

REMOTE-SENSING OF F-REGION ION DRIFTS AND ION TEMPERATURES AT SØNDRE STRØMFJORD, GREENLAND USING DOPPLER MEASUREMENTS OF THE $O^+(^2P)$ STATE

S.S. Carr

Department of Physics, The United States Air Force Academy

R. J. Niciejewski and T.L. Killeen

Space Physics Research Laboratory

Department of Atmospheric, Oceanic, and Space Sciences, The University of Michigan

Abstract. Ground-based observations of Doppler line profiles from the F-Region $O^+(^2P)$ state, made with the Fabry-Perot interferometer (FPI) at Søndre Strømfjord, Greenland have been analyzed to provide measurements of the ion convection velocity and ion temperature. The FPI line-of-sight (LOS) ion drift and temperature measurements have been compared with simultaneous incoherent scatter radar (ISR) measurements; the results from the two techniques are in good agreement.

Introduction

Ground-based Doppler measurements of F-Region ion drift velocities, using emissions from the $O^+(^2P)$ state, have been shown to be possible when the emission is sufficiently intense during nighttime hours (Smith et al., 1982; McCormac, 1984). This condition is satisfied at times in the polar cusp, polar cap, and other high-latitude auroral regions. At night, when the photoionization source at F2-Region altitudes is gone, the 7320Å emission may be observed only if energized by auroral electron impact ionization. At twilight, especially when the sun is ~ 1 -14° below the horizon, conditions for 7320Å emission observations are ideal since the F2-Region is still being photoionized, yet the ground is in darkness. Søndre Strømfjord, Greenland offers the experimenter both long hours of twilight and an auroral source for the 7320Å emission. During a September 1991 data campaign, ion drifts and temperatures were retrieved from twilight and aurorally produced 7320Å emissions. In this paper, we present the results of the data campaign. Incoherent scatter radar measurements will be compared with the co-located ground-based FPI (7320Å) drift and temperature measurements.

1. Aeronomy of the 7320Å Emission

The 7320Å doublet emission that is produced in twilight airglow and aurora is the result of the transition between excited ^2P and ^2D states of O^+ ions. These transitions occur at thermospheric heights and are strictly forbidden by electric dipole radiation; the transition probabilities are finite because of the existence of electric-quadrupole radiation (Chamberlain, 1961). The 7320Å emission doublets were initially studied to understand gaseous nebulae. Meriwether et al. (1974) found the individual components in the 7320Å doublet to be separated by about 0.8Å in an auroral study using a ground-based FPI. The components in the 7320Å doublet (Meriwether et al., 1978) are:

$$O^+(^2P_{3/2} \rightarrow {^2D_{5/2}}),\ \lambda = 7319.9\text{Å}$$

$$O^+(^2P_{1/2} \rightarrow {^2D_{5/2}}),\ \lambda = 7319.1\text{Å}$$

The two components of the 7320Å doublet are very closely spaced (~ 0.8Å) and most studies use the averaged wavelength. However, this quantity is heavily weighted in favor of the $O^+(^2P_{3/2} \rightarrow {^2D_{5/2}})$ component since the $O^+(^2P_{3/2} \rightarrow {^2D_{5/2}})$ component at ~7319.9Å is 3.8 times stronger than the $O^+(^2P_{1/2} \rightarrow {^2D_{5/2}})$ component at ~ 7319.1Å. Theoretical transition probabilities were first given by Seaton and Osterbrock (1957); they found radiative lifetimes of 4.57s for $O^+(^2P)$ ions and a branching ratio of ~0.781 for the ^2P - ^2D transition (Carr et al., 1992). The time taken for a newly-created ion to begin drifting with the bulk ion population in the **E**x**B** direction is very short (essentially given by the gyroperiod, which is ~ 0.2s). Since this is much shorter than the ion's radiative lifetime, it may be assumed that the Doppler shift of the emitted light is representative of the ion convection velocity.

Metastable $O^+(^2P)$ ions are primarily produced in the F2-Region by photoionization of neutral atomic oxygen by solar EUV radiation at wavelengths less than 666Å:

$$O + h\nu(\lambda < 666\text{Å}) \rightarrow O^+(^2P_{1/2}, {^2P_{3/2}}) + e$$

A secondary source of $O^+(^2P)$ ions is electron impact ionization, given by:

$$O + e \rightarrow O^+(^2P_{1/2}, {^2P_{3/2}}) + 2e$$

where the ionization threshold energy is 18.61eV.

$O^+(^2P)$ ions are lost by spontaneous emission or quenching. Spontaneous emission of the ions to lower states may be described as:

$$O^+(^2P) \xrightarrow{A_\lambda} O^+(^2D, {^4S}) + h\nu,\ A_\lambda = 0.219\,s^{-1}$$

where $A\lambda$ is the Einstein coefficient for spontaneous emission, in units of s^{-1}. The doublet emission at [OII] λ7320Å is produced by the following radiative transitions:

$$O^+(^2P_{1/2}) \xrightarrow{A_\lambda} O^+(^2D_{5/2}) + h\nu,\ A_\lambda = 0.020s^{-1},\ \lambda_1 \approx 7319.1\text{Å}$$

$$O^+(^2P_{3/2}) \xrightarrow{A_\lambda} O^+(^2D_{5/2}) + h\nu,\ A_\lambda = 0.077s^{-1},\ \lambda_2 \approx 7319.9\text{Å}$$

The following reactions are the major quenching losses of the $O^+(^2P)$ ion. These equations are listed with excess kinetic energy of the reaction and the currently accepted rate coefficients (Rees, 1989). Note that T_e denotes electron temperature.

$$O^+(^2P) + O \xrightarrow{k_O} O^+(^4S) + O + 5.0eV,\ k_O = 5.2\times10^{-11}cm^3s^{-1}$$

$$O^+(^2P) + N_2 \xrightarrow{k_1} N_2^+ + O + 3.02eV,\ k_1 = 4.8\times10^{-10}cm^3s^{-1}$$

$$O^+(^2P) + N_2 \xrightarrow{k_2} N^+ + NO + 0.70eV,\ k_2 = 1.0\times10^{-10}cm^3s^{-1}$$

$$O^+(^2P) + e \xrightarrow{k_3} O^+(^2D) + e + 1.69eV,$$

$$k_3 = 1.50\times10^{-7}\left\{\frac{300}{T_e}\right\}^{1/2} cm^3s^{-1}$$

$$O^+(^2P) + e \xrightarrow{k_4} O^+(^4S) + e + 5.0eV,$$

$$k_4 = 4.0\times10^{-8}\left\{\frac{300}{T_e}\right\}^{1/2} cm^3s^{-1}$$

Paper number 93GL01966
0094-8534/93/93GL-01966$03.00

The production rate of $O^+(^2P)$ ions, assuming equilibrium conditions, is

$$P = [O^+(^2P)]\{0.219 + k_e[e] + k_{N_2}[N_2] + k_O[O]\}$$

The volume emission rate for any transition is defined as

$$\eta = A[X]$$

where η is the emission rate, A is the Einstein coefficient and [X] is the concentration of species X. Using the above two equations, one can determine the volume emission rate in the 7320Å doublet above ~180km to be:

$$\eta_{7320Å} = \frac{0.097P}{\{0.219 + k_e[e] + k_{N_2}[N_2] + k_O[O]\}} \approx 0.44P$$

where 0.097 is the sum of the two Einstein coefficients for the transitions in the 7320Å doublet. Above the quenching zone (~180km), all terms in the denominator are small with respect to the quenching loss term (0.219), and one is therefore left with 0.44P. Below ~180km, the $O^+(^2P)$ ions are severely quenched and the 7320Å emission is difficult to detect.

2. FPI

The FPI at Søndre Strømfjord uses a 12 channel image plane detector (IPD), 10cm diameter etalon with a 1.116 cm gap between the plates, and a six-channel tilting filter selector. The instrument has a spectral resolution of 0.01Å with an instrumental drift less than 0.0002Å/h (or ~10 m/s). The 7320Å filter used in this study has a bandpass of 3.5Å (thereby isolating the 7320Å emission from the $P_1(2)$ rotational line of the OH (8-3) molecular band at ~ 7316Å and from the $O^+(^2P)$ 7330Å doublet emission) with a maximum transmission at 7320.1Å and peak transmission of 59%; the peak of the measured 7320Å profile was optimized at channel 5 of the IPD at an etalon pressure of ~15.3 psi. The Søndre Strømfjord FPI separated the 7320Å doublet components on the image plane detector by ~ 6 channels, with the weaker line of the doublet appearing near channel 11 (Carr, 1992).

Presently, the FPI at Søndre Strømfjord operates in a cyclic mode observing OI (5577Å) and OI (6300Å) emissions in the zenith and the four geographic cardinal directions (at an elevation angle of 45°). There is also a calibration mirror position where a neon lamp is sampled once every cycle to record instrument drift through the night. A 300s dark count is recorded each cycle to monitor background counts induced by electronic noise. Each cycle takes ~20 minutes to complete. The instrument function of the FPI is determined regularly by performing a pressure scan of a frequency stabilized He-Ne laser. This experiment characterizes the broadening functions caused by the instrument and allows the source profile to be determined from the measured profile. The wind and temperature analysis is similar to that described in Nardi (1991); the analysis is performed on every fringe retrieved during the night. Once this is complete, the ion drifts must be corrected further to account for instrument drift during the night. The drift is removed from the derived ion drift by fitting a spline function through the calibration values for the entire night and subtracting the calibration ion drift velocity corresponding to the time of the individual measurement. A reference wavelength of channel position corresponding to zero velocity is obtained empirically and depends on the assumption that over the period of a night the average of the derived vertical velocities is zero. During the 3 - 10 Sep 91 data campaign, the FPI cyclic mode was extended to include 7320Å observations, providing a set of ion drifts and temperatures.

3. Incoherent Scatter Radar (ISR)

Co-Located with Michigan's FPI at 66.59°N, 50.95°W (74° invariant latitude) is the ISR; it has a transmitting frequency of 1290MHz (23cm) and is fully steerable, allowing for a variety of operating modes. A number of pulse schemes may be used; in this study, the long pulse (320μs) scheme was used. The long pulse scheme is best suited for F-Region and topside plasma measurements because it provides the best signal to noise ratio. During the September 1991 campaign, data were recorded with two different antenna modes. One mode directed the receiving antenna pattern up-**B** (up the magnetic field line) for four minutes and at two other positions for two minutes each; the other mode was dwelling up-**B** indefinitely. The data were integrated in time for as long as the antenna dwelled at a position in the three position mode or for 5 minutes if the antenna were in the up-**B** mode. The resulting range resolution, with a radar pulse length of 48km, was ~42km in the 200 - 400 km zone of the ionosphere.

Plasma properties can be determined by examination of the backscattered radar signal. The backscattered power spread over a range of frequencies is caused by Doppler shifting of the radar wave as it is scattered by waves in the plasma. This return is the power spectrum. Analysis of this spectrum can directly yield electron density, line-of-sight ion velocity, electron temperature, ion temperature, ion-neutral collision frequency and ion composition.

4. Results and Discussion

The desired conditions for making the FPI (7320Å) emission observations at Søndre Strømfjord occur at twilight with the solar depression angle between ~ 4 - 14°, clear skies (scattering from clouds may alter the spectral information of the emission), or nighttime (Rayleigh scattered light must be avoided since it obscures the weak nightglow) with no discrete aurora in the field-of-view. Discrete aurora originate at various heights; hence, the resulting FPI measurements cannot be attributed to a certain altitude. No discrete aurora were in the field-of-view during the observations presented in this paper. When clouds are present, the background signal strength increases substantially. For the 7320Å emission, we found that sky cover had to be two octa or less or the background would become intolerable. During two nights of observations, the sky cover increased to greater than this value, and we ignored the data with poor signal to noise characteristics. The condition necessary for ISR measurements is that there must be at least ~ 10^5 electrons/cm^3 at F-Region altitudes.

Figure 1 is an illustration of analyzed data from Søndre Strømfjord's FPI (7320Å) for the night of 3/4 Sep 91. Universal Time and the appropriate 3-hourly kp is the abscissa for all panels. The Ap and F10.7 indices for this period were 15 and 171 respectively. Observations began once the solar depression angle exceeded ~4°, which for this time of year was from ~ 20UT to 08UT. Each measurement is indicated by its corresponding first initial (N ~ north) along with its error bar in each of the panels. The upper two panels contain the retrieved FPI (7320Å) meridional and zonal ion drifts in m/s, after accounting for elevation angle, instrument drift and the zero wind reference. Positive is the standard convention: north and east. Since the FPI observed at an elevation angle of 45°, the north and south measurements are therefore separated by ~ 500 km, assuming an emission altitude of ~250 - 300 km; this distance corresponds to ~ 5° in latitude.

Unlike neutral winds, these ion drifts show considerable fluctuation between successive meridional and zonal measurements, indicating that the ion drifts in the high latitude ionosphere change significantly over 5° of latitude. OI (6300Å) measurements show the meridional and zonal measurements to be nearly identical (Thayer, 1990). In these ion measurements, the drifts change considerably in 5° of latitude and strong areas of plasma convergence and divergence are seen in Figure 1. Referring to Figure 1, the bottom left panel contains the FPI (7320Å) ion temperatures

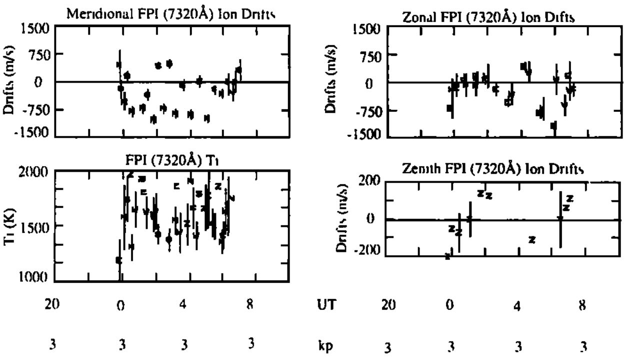

Fig.1 Analyzed data from the Søndre Strømfjord FPI (7320Å) for 3/4 Sep 91. See text for discussion.

for each measurement with corresponding error bars. The bottom right panel contains the vertical ion drifts. During the 3 - 10 Sep 91 campaign, the vertical ion drift velocities ranged from -200 to 100 m/s and averaged to zero.

Further analysis of the high latitude ion drift convection pattern made by a ground-based FPI may be done by comparing experimental results to theoretical and empirical model output. The Vector Spherical Harmonics (VSH) model is a computer subroutine that describes the composition and dynamics of the thermosphere and ionosphere from 130 - 600km (Killeen et al., 1987). In Figure 2, we have run the VSH model for the exact geophysical conditions that took place on 4 Sep 91 at 01 UT at Søndre Strømfjord. Figure 2 is a satellite view of the earth from two earth radii; a cross-hair is placed near Søndre Strømfjord for identification. The drift barb in the bottom right corner represents 1000 m/s. One can see that a southeastward flow of ion drifts of about 700 m/s and an ion temperature of about 1320K is the output near Søndre Strømfjord. Referring to Figure 1, one sees an observed meridional (south) flow of ~ 700-750 m/s (these speeds straddle 01UT), an observed zonal (east) flow of ~ 10 m/s (the resultant velocity flow is southeastward at ~ 725 m/s) and an observed temperature of ~ 1300 - 1600K (these temperatures straddle 01UT). These observed values favorably agree with the VSH output. VSH runs for other time periods during this data campaign produced favorable comparisons.

Comparisons between the ISR and FPI were difficult to make, mainly because of different integration times, sensing

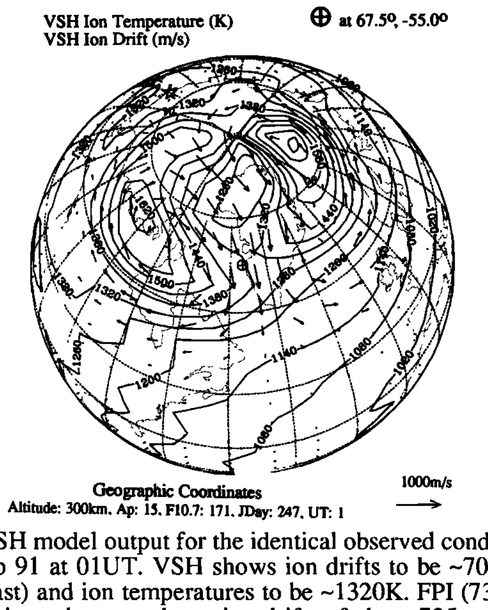

Fig.2 VSH model output for the identical observed conditions of 4 Sep 91 at 01UT. VSH shows ion drifts to be ~700 m/s (southeast) and ion temperatures to be ~1320K. FPI (7320Å) observations show southeast ion drifts of about 725 m/s and ion temperatures of ~1300 - 1600K.

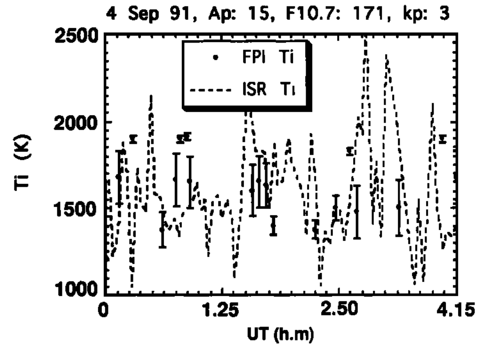

Fig.3 FPI (with error bars) vs ISR (dash line) ion temperature comparison for 4 Sep 91. The integration period for the ISR was usually much shorter than that of the FPI, resulting in greater resolution in the ISR measurements. Generally, the agreement is good, suggesting future study of this emission at pre-determined times and seasons could prove eventful in understanding ionospheric energetics.

locations and fields-of-view. The FPI patrols consisted of integration times varying from ~ 120 to 720 seconds. The ISR normally had integration times of about 120 seconds. In Figure 3, we overplot ISR and FPI temperature values. Agreement is reasonable. For ion drift velocity components, the ISR data were bin averaged so their lines-of-sight and integration times matched those of the FPI drifts. We then plot an ISR error which is simply a standard deviation about the mean. From Figure 4, one can see that the drift comparison (zonal, in this case) seems to be reasonable. FPI-North and FPI-South (meridional) measurements were sometimes found to be considerably different from ISR measurements. This was due to the fact that as the auroral oval moves over Søndre Strømfjord during the evening, spatial and temporal changes in the oval are occuring quicker than the FPI integration times. Figure 5 is a sum of the FPI (7320Å) drift components combined into vector form and plotted on a geographic polar dial. The drift barb on the lower left corner of the plot represents 500 m/s. Times are local solar and the circles start at 60°N geographic latitude and move inward to the North Pole. We have assumed that the 7320Å emissions originate from ~ 300 km.

The solar wind's electric field is mapped into the polar cap ionosphere along geomagnetic field lines of equipotential, where a dawn-dusk electric field will result. This electric field drives the polar ionospheric F-Region plasma in the antisunward direction at a drift velocity given by

$$\vec{V}_d = \frac{\vec{E} \times \vec{B}}{|B|^2}$$

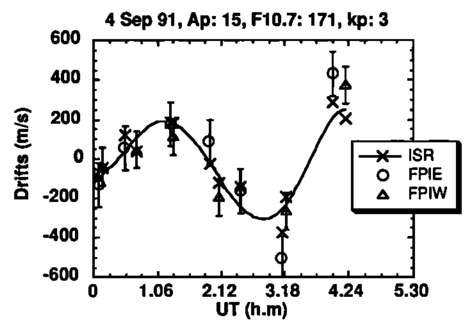

Fig.4 ISR (X's with 5th-order polynomial curve fit through points) vs FPI (with error bars) ion drift comparisons. FPIE(W) indicates the FPI was looking eastward (westward). The ISR data were bin averaged so their lines-of-sight and integration times matched those of the FPI (7320Å) drifts. The comparison between the FPI (7320Å) and ISR drifts is good.

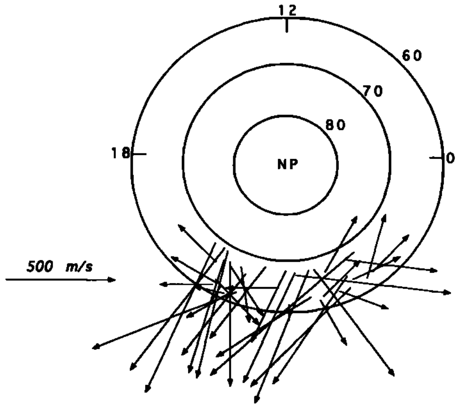

Fig.5 Polar dial plot for four nights of FPI (7320Å) ion drift observations. A pattern consistent with a two-celled ion convection pattern is visible, complete with antisunward flow seen in the center of the bottom dial and return flow seen on either side. The times on this dial are local solar and the latitudes are geographic.

where the geomagnetic field is directed into the page in Figure 5. The sign of the electric field in reversed in the auroral zone; there, the resulting ion flow is sunward. A pattern consistent with a two-celled ion convection pattern is apparent in Figure 5 from just four nights of ground-based observations. Antisunward flow is seen in the center of the bottom dial, with the beginnings of return flow on either side.

5. Conclusions

The first ion convection pattern measurements and ion temperature measurements using an FPI (7320Å) from Søndre Strømfjord have been presented and compared to simultaneous ISR measurements. The agreement is good, although a limited dataset of four nights exists. Comparisons to the Vector Spherical Harmonic (VSH) model are good, but the grid size of the model is too large and four nights of FPI data are too sparse to give precise comparisons. The FPI and ISR are complementary diagnostic experiments - they rarely point in the same place for the same length of time. Theoretical and empirical models, such as VSH, only supply our best guess as to geophysical conditions. Our FPI measurements permit fine tuning of the models.

Making 7320Å emission observations on a regular basis will provide needed information on the high latitude ion convection pattern, ion outflow, and ionospheric energetics. The method of observation is simple, inexpensive and proven. The low intensity (~20-100R) and sporadic nature of the 7320Å emission in nighttime aurorae currently limit ground-based FPI observations. However, the addition of a CCD detector would enhance the Søndre Strømfjord capabilities immensely. With a CCD, one could more easily record this weak emission and use shorter FPI integration times, thereby generating more frequent ion drift and ion temperature measurements. The resulting larger database of ion drifts and temperatures will give us a more complete understanding of high-latitude ionospheric and thermospheric dynamics and energetics.

Acknowledgements. This work was supported by NSF Grant ATM-8901367. S. S. Carr is funded by the US Air Force. The authors wish to thank the Søndre Strømfjord radar site crew for their assistance during the data campaign.

References

Carr, S.S., T.L. Killeen and W.R. Coley, Remote-Sensing Observations of F-Region Ion Drift Velocities Using Dynamics Explorer-2 Doppler Measurements of the $O^+(^2P)$ λ732.0 nm Emission, Geophys. Res. Lett., 19, 1455, 1992.

Carr, S.S., Observing and Modelling F-Region Ionospheric Dynamics Using the [OII] 7320Å Emission, PhD Thesis, The University of Michigan, 1992.

Chamberlain, J.W., Physics of the Aurora and Airglow, Academic Press, 1961.

Killeen, T.L., R.G. Roble, N.W. Spencer, A Computer Model of Global Thermospheric Winds and Temperatures, Adv. Space Res., 7, 207, 1987.

McCormac, F. G., An optical investigation of ion and neutral motions in the polar thermosphere, PhD Thesis, Ulster Polytechnic, 1984.

Meriwether, P.B. Hays, K.D. McWatters, A.F. Nagy, Interferometric Measurements of the λ7319Å Doublet Emission of OII, Planet. Space Sci., 22, 636, 1974.

Meriwether, J.W., D.G. Torr, J.C.G. Walker, A.O. Nier, The $O^+(^2P)$ Emission at 7320Å at Twilight, J. Geophys. Res., 83, 3311, 1978.

Nardi, B., An Inversion Technique to Recover Lower Thermospheric Winds from Space-borne Remote Measurements of [OI] 5577Å, PhD Thesis, The University of Michigan, 1991.

Rees, M.H., Physics and Chemistry of the Upper Atmosphere, Cambridge University Press, 1989.

Seaton, M.J., Osterbrock, R.E., Relative OII Intensities in Gaseous Nebulae, Astrophys. J., 126, 66, 1957.

Smith, R. W, G. G. Sivjee, R. D. Stewart, F. G. McCormac, and C. S. Deehr, Polar Cusp ion drift studies through high-resolution interferometry of O^+ 732.0 nm emission, J. Geophys. Res., 87, 4455, 1982.

Thayer, J.P., Neutral Wind Vortices in the High-Latitude Thermosphere, PhD Thesis, The University of Michigan, 1990.

S. S. Carr, Department of Physics, US Air Force Academy, Colorado Springs, CO; R.J. Niciejewski and T. L. Killeen, Space Physics Research Laboratory, Department of Atmospheric, Oceanic and Space Sciences, The University of Michigan, 2455 Hayward, Ann Arbor, MI 48109.

(Received: May 18, 1993;
accepted: July 13, 1993)